Molecular Crystals and Liquid Crystals Science and Technology. Section A. Molecular Crystals and Liquid Crystals

Publication details, including instructions for authors and subscription information:
http://www.tandfonline.com/loi/gmcl19

Photo-Induced Space Charge Fields, Photo-Voltaic, Photorefractivity, and Optical Wave Mixing in Nematic Liquid Crystals

I. C. Khoo [a] , Brett D. Guenther [a] & S. Slussarenko [b]

[a] Department of Electrical Engineering, Pennsylvania State University, University Park, PA, 16802, USA

[b] Institute of Physics, Ukrainian Academy of Sciences, Prospect Nauki 46, Kiev-22, 252650, Ukraine

Version of record first published: 24 Sep 2006

To cite this article: I. C. Khoo, Brett D. Guenther & S. Slussarenko (1998): Photo-Induced Space Charge Fields, Photo-Voltaic, Photorefractivity, and Optical Wave Mixing in Nematic Liquid Crystals, Molecular Crystals and Liquid Crystals Science and Technology. Section A. Molecular Crystals and Liquid Crystals, 321:1, 419-438

To link to this article: http://dx.doi.org/10.1080/10587259808025107

Mol. Cryst. Liq. Cryst., Vol. 321, pp. 419–438
Reprints available directly from the publisher
Photocopying permitted by license only

Photo-Induced Space Charge Fields, Photo-Voltaic, Photorefractivity, and Optical Wave Mixing in Nematic Liquid Crystals

I. C. KHOO[a], BRETT D. GUENTHER[a], and S. SLUSSARENKO[b]
[a]Department of Electrical Engineering, Pennsylvania State University, University Park, PA 16802, USA; [b]Institute of Physics, Ukrainian Academy of Sciences, Prospect Nauki 46, Kiev-22, 252650, Ukraine

We present a detailed discussion of the fundamental mechanisms for recently observed nonlinear electro-optical wave mixing effects in nematic liquid crystal films. Experimental results on photoconductivity, photorefractive-like two beam coupling, beam amplification, self-diffraction, and storage holographic grating formation in dye- and Fullerene C_{60} and C_{61} doped nematic films are presented along with a review of two- and four- wave mixing theories. Nematic liquid crystal films are shown to be potentially useful for adaptive and optical storage applications.

Keywords: photorefractivity; photo-voltaic; wave mixing; beam amplification; fullerene; nematic; adaptive optics; holographic grating; storage; light valve

INTRODUCTION

Nematic liquid crystal films containing photo-excitable dopants exhibit numerous interesting nonlinear optical phenomena. In particular, recent studies[1-6] have shown that a linearly polarized laser could create a DC space charge field, which in combination with a bias DC field, creates a director axis reorientation. This process gives rise to a very large change in the refractive index under very low optical power (i.e. an extraordinarily large optical nonlinearity). Since the main underlying physical parameter for the index modulation is the optically induced space charge fields, analogous to

the well known photorefractive effect in ferrorelectric materials[7], this effect observed in the nematic liquid crystal has been termed an orientational photorefractive effect.[2,3] The phenomena is now quite well documented, but new and interesting and potentially useful features continue to emerge from recent studies.

Consider the interaction geometries as shown in Figures 1a and 1b, involving two coherent laser beams overlapping on the nematic films.

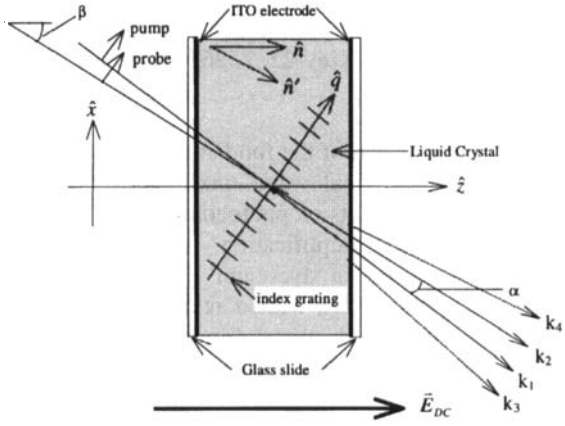

FIGURE 1a Schematic depiction of coherent optical wave mixing in a homeotropically aligned nematic liquid crystal film.

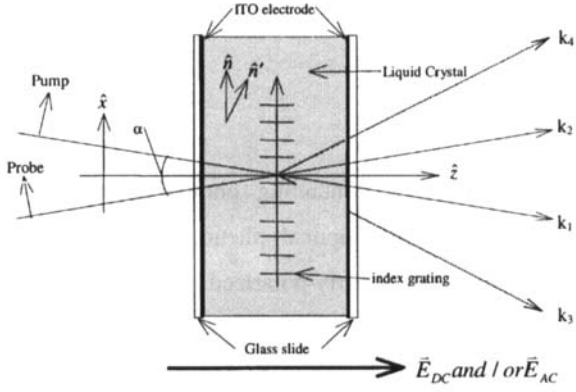

FIGURE 1b Schematic depiction of coherent optical wave mixing in a planar aligned nematic liquid crystal film.

The space charge fields result from several mechanisms. The first such mechanism is analogous to those found in typical photorefractive crystals[1-7], in which the photo-induced ions are redistributed via diffusion, migration, and/or the action of the applied DC field. The other two mechanisms[2,3] are unique to nematic liquid crystals and are attributed to the dielectric and conductivity anisotropies and the ability of the nematic liquid crystals to flow.

In this paper, we give a review of these electro-optical processes, and present recently obtained optical wave mixing results such as asymmetric self-diffraction, aberration-free beam amplification, and high resolution holographic grating formation. We also report the first observation of optically produced DC voltage in a particular methyl red doped nematic liquid crystal film.

SPACE CHARGE FIELDS AND REFRACTIVE INDEX CHANGES

As mentioned above, there are three principle sources of space charge fields. For incident optical intensity of the form $I_{op} = I_o\left[1+m\cos(q\cdot r)\right]$ the photorefractive-like space charge field is given by[1]:

$$E_{ph} = \frac{mk_B T}{2e} qv \frac{\sigma - \sigma_d}{\sigma} \sin(\vec{q}\cdot\vec{r}) \tag{1}$$

where k_B = Boltzman constant, σ = illuminated state conductivity, σ_d = dark state conductivity,

$$v = \frac{D^+ - D^-}{D^+ + D^-} \tag{2}$$

where D^+ and D^- are the diffusion constants for the positively and negatively charged ions, respectively. The constant m is the optical intensity modulation factor.

Notice that E_{ph} is $\pi/2$ phase shifted from the incident optical intensity function. Therefore, the director axis reorientation is also phase shifted with respect to the optical intensity function. This phase shift is responsible for the first reported[2] observation of the two-beam coupling effect.

As first pointed out by Khoo,[2,3] two other sources of space charge fields also contribute to this effect. They arise from the conductivity and dielectric anisotopies present within the nematic liquid crystal film. The fields can be shown to be[3]:

$$E_{\Delta\sigma} = \frac{-(\sigma_{\parallel} - \sigma_{\perp})\cos\theta\sin\theta}{\sigma_{\parallel}\sin^2\theta + \sigma_{\perp}\cos^2\theta}E_z \sim \frac{-\Delta\sigma}{\sigma_{\perp}}\theta E_z \text{ (For small } \theta) \qquad (3)$$

$$E_{\Delta\varepsilon} = \frac{-(\varepsilon_{\parallel} - \varepsilon_{\perp})\cos\theta\sin\theta}{\varepsilon_{\parallel}\sin^2\theta + \varepsilon_{\perp}\cos^2\theta}E_z \sim \frac{-\Delta\varepsilon}{\varepsilon_{\perp}}\theta E_z \text{ (For small } \theta) \qquad (4)$$

where $\Delta\sigma = \sigma_{\parallel} - \sigma_{\perp}$ is the conductivity anisotropy and $\Delta\varepsilon = \varepsilon_{\parallel} - \varepsilon_{\perp}$ the dc dielectric anisotropy.

These space charge fields are proportional to the applied DC field, E_z. For small displacement angles, the space charge fields are proportional to the angle itself. Thus a small initial reorientation angle and a space charge field with reinforce each other until they reach a steady state value. Once the reorientation is established, the space charge field can be maintained by the DC field alone, without the need for any optical fields. This behavior was confirmed in our reported study[3,5] of the dynamics of holographic grating formation.

Since these space charge fields are functions of the reorientation angle θ, its spatial phase shift with respect to the optical intensity function depends on the originating mechanism for θ. If θ originates from the photorefractive effect, the phase shift will be $\pi/2$. If the reorientation is due to some other local effect, such as the optically induced director axis reorientation, then the phase shift will be different.

In summary, there are three mechanisms for (extraordinary wave) refractive index changes associated with director axis reorientation in the nematic film under the application of an optical field plus a DC bias field. These mechanisms are outlined as follows:

(1) Charge generation → ions drift/diffusion → charge separation and space charge field formation → director axis reorientation → refractive index change.
(2) Charge generation → ionic conduction plus director axis reorientation → space charge field formation through dielectric and conductivity anisotropies → further director axis reorientation → refractive index change.
(3) Charge generation → material flows → velocity gradient and shear stresses → director axis reorientation → refractive index change.

DYE, C60, AND C61 DERIVATIVE DOPED NEMATIC FILMS

All three processes outlined above involve the basic mechanism of photo-charge production. Since the incident photonic energy, hν, is less than the ionization potentials of the dopant and the impurity molecules in the liquid crystals, the photo-charge production is attributed to excited state photochemical processes. In the case of R6G dye, or other laser dye molecules, studies[8] have shown that the ions are generated by dissociation. In C_{60} molecules, the formation of charge transfer complexes[9] is the likely cause of charge production. Some hitherto undetermined electro-chemical processes may also play a role in the persistent holographic process, as evidenced by the observed difference in the grating storage times for different doped NLC films. In the R6G dye doped NLC samples, a written grating can last for tens of minutes, while a grating written in a C_{60} doped NLC sample persists indefinitely.[2,3]

We have investigated the photo-charge production of a variety of dopants, including several laser dyes (R6G, methyl red, etc.), dichroic dye, and Fullerenes (C_{60}, C_{70}, and derivatives). It was found that C_{60} and its derivative, C_{61}, are among the best dopants in terms of photo-charge production. The results are shown in Tables 1 and 2.

TABLE 1: Photo-induced current in 100 μm thick homeotropically aligned nematic films; (single beam) laser power = 100 mW; beam diameter = 2 mm; DC voltage = 1 volt; $\lambda = 514.5$ nm

DOPANT	D2	R6G	C60	UNDOPED
Concentration by weight	0.5%	0.2%	0.05%	NA
I_{dark} ($\times 10^{-8}$ Amps)	3.5	2.9	6.0	0.5
$I_{illum.}$ ($\times 10^{-8}$ Amps)	4.2	13	13	0.5
ΔI ($\times 10^{-8}$ Amps)	0.7	10	7	<0.1
α (cm^{-1})	373	102	30	20
$\Delta I/\alpha$ ($\times 10^{-11}$ amp-cm)	1.9	99	230	<5

TABLE 2: Photoinduced current in 25 μm thick homeotropically aligned nematic films, (single beam) laser power = 20 mW; beam diameter = 2 mm; DC voltage = 1 volt; $\lambda = 514.5$ nm

DOPANT	C60	C61*	C60+C70
Concentration by weight	0.05%	0.12%	1%
I_{dark} (mA)	0.120	0.3	1
$I_{illum.}$ (mA)	0.145	0.315	1.05
ΔI (mA)	0.025	0.015	0.05
α (cm^{-1})	4	1.2	4.8
$\Delta I/\alpha$ (mA-cm)	0.0063	0.0125	0.01

OPTICAL WAVE MIXING EFFECTS

We have recently studied several new aspects of transient and storage optical wave mixing processes in doped NLC films. As shown in Figures 1a and 1b, the linearly polarized, mutually coherent pump and probe beams are overlapped on the NLC films at a small wave mixing angle, α. The liquid crystal typically used in our experiments is 5CB (Pentyl Cyano Biphenyl) with traces of Fullerene C_{60} (0.05% by weight) dissolved in it. However, pure undoped 5CB films were also tested. The sample thicknesses range from 6 to 25 microns. The glass slides are coated with a transparent electrode (ITO) so that a uniform electric DC and/or AC field could be applied to the NLC film. The laser used in the experiments is a Argon-ion laser tuned to either the 488.0 nm or the 514.5 nm wavelength. The pump/probe beam ratio was adjusted by an attenuator placed in the path of the signal beam, while the pump power was made variable through the use of a pair of polarizers. The beam diameter at the sample is 3mm.

Self Diffraction in Homeotropically Aligned NLC Films

For the homeotropically aligned NLC sample, the film is tilted such that the beam propagation direction makes an angle, β, with the director axis. The occurrence of wave mixing effects and their dependence on the applied DC voltages and incident beam directions are similar to those reported before.[2,5] In particular, visible amplification of the probe beam and the generation of side diffractions are observable for an applied DC voltage greater than 1.5 volts.

Monitoring the self-diffraction under an equal pump/probe beam ratio gives a vivid depiction of the energy flow between the pump and the probe beams. In the NLC sample one beam grows at the expense of the other beam

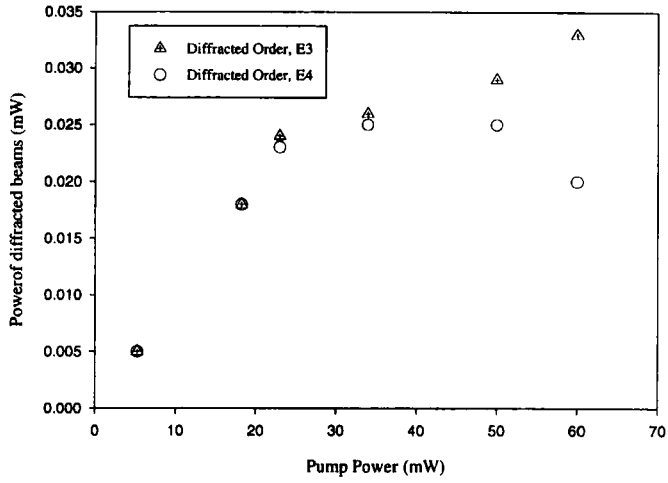

FIGURE 2a: Self-diffractions as a function of the total input power (pump + probe) for an undoped nematic (5CB) film. DC voltage = 3V, film thickness = 25 μm.

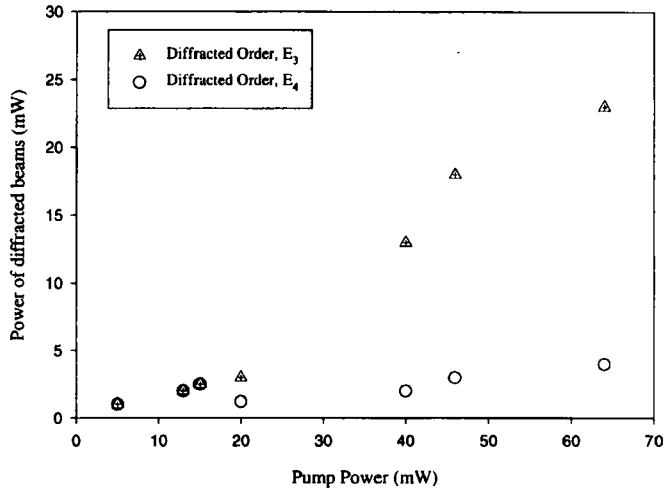

FIGURE 2b: Self-diffractions as a function of the total input power for an C_{60} doped nematic (5CB) film. DC voltage = 3V, film thickness = 25μm.

due to the energy coupling between the two beams. As shown in Figures 2a and 2b, for undoped and C_{60} doped films, the beam energy transfer increases dramatically with the input optical intensity. The input beams as well as the diffracted orders begin to deviate from unity ratio. As expected, this "divergence" is more pronounced in the C_{60} doped sample (c.f. Figure 2b).

For a given dopant, the wave mixing efficiency is highly dependent on the grating spacing and the film thickness. From equation (1), we note that the photorefractive space charge fields increase as the grating spacing is reduced; also the DC field is proportionally enhanced if the sample thickness is reduced, for a given applied DC voltage. This dependence is opposite to the director axis reorientation process, which is diminished by larger elastic torques for smaller grating spacing and/or film thickness.[10] Accordingly, there is an optimum grating spacing value for the diffraction efficiency. As shown in reference [3], the grating spacing for optimal wave mixing effect is on the order of twice the film thickness. This is again demonstrated in our recent studies of self-diffraction in a 6 μm think C_{60}-doped film (c.f. figure 3). Note that the diffraction is maximal at a grating spacing of nearly twice the film thickness.

An important finding from these studies of thin films is that very small optical intensity is required to generate substantial self-diffraction. In C_{60} or Methyl-red doped samples, we have observed that diffraction of a few percent can be generated with an input optical intensity of $\leq 200\ \mu W/cm^2$. This sensitivity rivals those obtainable from liquid crystal light valves[10,11] and other photorefractive devices.[7]

In Methyl-red doped homeotropic samples, we observe that self-diffraction can be generated without the application of the DC-field, with an input optical power of less than 1 mW/cm^2.

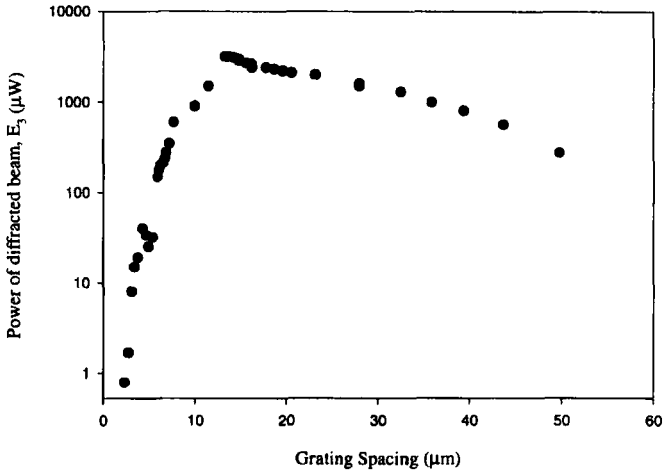

FIGURE 3: Dependence of the diffraction efficiency on the grating spacing for a permanent grating formed in a C60 doped nematic film. The film thickness=6 microns, P_{laser}= 30 mW, λ= 448 nm, beam dia.= 1cm, and V_{dc} = 3 V

With the application of a DC field, the wave mixing efficiency is enhanced by more than an order of magnitude. Self-diffraction of a few percent can be generated with an input optical power density of ~200 μW/cm^2. Furthermore, the response time of the self-diffraction can be shortened to 100 msec regime with the applied DC field. This unusual response of the methyl-red doped sample is attributed to the photo-induced DC voltage, a photo-voltaic effect, which will be discussed in more detail in a later section.

Self Diffraction in Planar Aligned NLC Films

For the planar aligned samples, the input beams in the self diffraction experiment are symmetrically incident on the film, and an AC field is applied to the sample to pretilt the director axis. Alternatively, one can also tilt the sample physically to obtain effects similar to the homeotropically aligned sample.

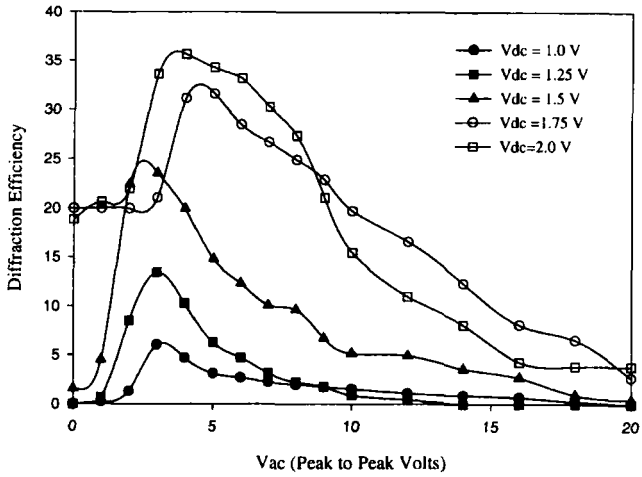

FIGURE 4: Diffraction efficiency as a function of the AC and DC voltage for a C_{60} doped NLC (5CB) film. Power= 40 mW (for both the pump and probe), λ=514.5 nm, and sample thickness = 25 μm.

Figure 4 shows the dependence of the first order self-diffraction, E_3, on the applied DC and AC fields for the geometry shown in Figure 1b. Below the Freedericksz transition voltage, the director axis is parallel to the optical electric field and there is no significant diffraction. As the voltage across the sample is increased the diffraction power increases until it reaches a maximum value, similar to the homeotropic case where maximal refractive index modulation due to director axis reorientation occurs at β=45°. As the AC voltage is further increased the diffraction power decreases because the molecules are now strongly aligned with the AC field (i.e. perpendicular to the cell boundary), thereby diminishing the photorefractive effect. Under higher DC bias voltage, persistent gratings are formed in the short time it takes to acquire data. This effect can be seen in Figure 4 (V_{dc}=1.75 and V_{dc}=2.0). The data for this figure was acquired by starting at a high AC voltage and working backwards to a zero AC voltage while the DC voltage is

applied. The diffraction at an AC voltage of zero signifies the presence of a persistent grating. These persistent gratings can be "switched" on or off by applying a large AC field[3]. Persistent gratings will be discussed further in a later sections.

Although the use of an AC field (above the Freedericksz field transition) in the case of planar sample appears somewhat cumbersome, it nevertheless allows the observation of the photorefractive effect in a normal incidence geometry (i.e. β=0). This feature is important for potential light valve like applications of this photorefractive nematic liquid crystal.

Beam Amplification Theory and Experiments

The process of energy transfer between the two input beams is complicated by the presence of side diffraction beams (i.e. E_3, E_4, etc.). Such multiwave mixing processes have been quantitatively analyzed by Khoo and others[6,12,13] in their study of purely optically induced director axis reorientation in NLC films. Following their multiwave mixing theory modified accordingly for a phase-shifted index grating,, the equation for the three optical electric fields E_i involved (i.e. pump=E_1, probe=E_2, and diffraction on the pump side=E_3) are given by:

$$\frac{dE_1}{dz} = -g\left[\left(E_1E_2^*\right)E_2 + \left(E_1E_3^*\right)E_3 + other\_wavemixing\_terms\right] \tag{5}$$

$$\frac{dE_2}{dz} = g\left[\left(E_2E_1^*\right)E_1 + \left(E_1E_3^*\right)E_1e^{i\Delta kz} + other\_wavemixing\_terms\right] \tag{6}$$

$$\frac{dE_3}{dz} = g\left[\left(E_3E_1^*\right)E_1 + \left(E_1E_2^*\right)E_1e^{i\Delta kz} + other\_wavemixing\_terms\right] \tag{6}$$

In these equations, g, is the real coupling constant, whose sign depends on the direction of the applied DC field.[2,3] The factor $\Delta k = |2k_1 - k_2 - k_3|$ is the wave vector mismatch with k_i being the magnitude of the i^{th} optical wave vector along the z direction. At large pump/probe beam ratio (i.e. very weak probe beam) the diffracted beam E_3 is relatively much weaker than E_2, and higher order diffractions (E_4, E_5, etc) are negligibly small. This justifies the consideration of only three interacting waves.

The two terms on the right hand side of these equations describe the wave mixing contribution from the gratings formed among the two incident beams E_1, E_2 and the first order diffracted beam E_3 on the pump side. Note that $E_2 E_1^* E_1$ is independent of the phase (and therefore any phase aberration) of the pump beam since it is proportional to $E_1^* E_1$. On the other hand, the latter term $E_1 E_3^* E_1 e^{i\Delta k_2 z}$ will impart phase aberration on the amplified probe beam, since it is proportional to $E_1 E_1$. To achieve aberration-free amplification, this term should be suppressed, either by using a very weak probe, or using a thick film so that the wave mixing process is in the Bragg regime($\lambda d >> \Lambda_g^2$), where d = sample thickness and Λg is the grating spacing. This is indeed demonstrated in experiments using a weak probe beam, and reported in reference [6].

The wave mixing beam amplification process has transient and storage features. If the exposure time is short (a few seconds), the effect is transient. Figure 5 shows the probe gain (2 seconds after the application of the external DC field) as a function of the DC voltage appearing across a 25 micron thick C_{60} doped homeotropically aligned nematic film. The pump/probe beam ratio used was 239.

In experiments with a 10 micron sample, a probe gain value of ~18 was obtained.[6] Here gain was defined as the ratio of the transmitted probe with

external fields on to the transmitted probe power without fields. This gain corresponds to an exponential gain constant of 2890 cm^{-1}. Such large gain is attributed to the use of more photo-conductive dopants such as C_{60} rather than relying on the photo-conductive properties of unknown impurities in commercially "pure" liquid crystals used in previous wave mixing experiments[2], where the gain achieved was much smaller. The high gain can also be explained by the large DC field strengths present in thin samples. Since the space charge fields are proportional to DC field strength thin samples should have a more pronounced photorefractive effect than thicker ones.

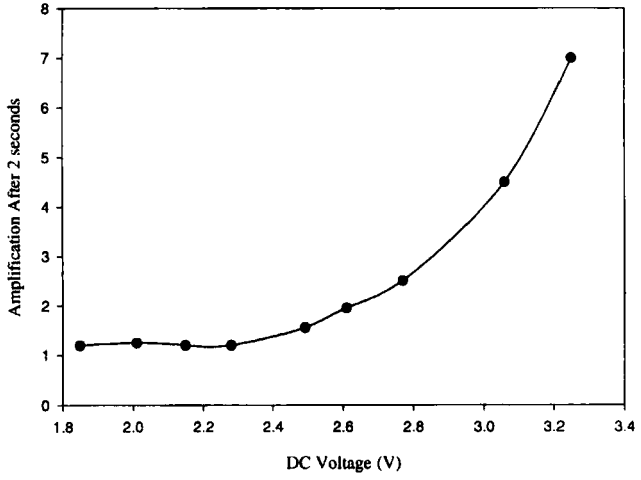

FIGURE 5: Transient probe beam amplification for short exposure time (2 seconds) at a wavelength of 488nm, α = 1 degree, β ~ 22.5 degrees, pump beam power = 98 mW.

Grating Storage Capability

If the applied DC field and the incident beams are left on for a sufficiently long time (~ 1 minute), the amplified probe and the pump beam will create a

permanent grating on the sample. Starting with a very weak probe beam (pump/probe beam ratio > 200), the steady state situation consist of a highly amplified beam, several orders of diffraction, and a permanent grating that can be turned on/off by an externally applied AC field.[3]

Our previous investigation[3] and theories have shown that the storage grating efficiency is dependent on the grating spacing as well as the sample thickness, similar to the transient case. Figure 6 shows a recently obtained dependence of the stored grating diffraction efficiency on the grating constant for an 6 μm thick undoped 5CB NLC film. Notice that the diffraction efficiency peaks at a grating wavelength of about two times the film thickness. These results are in agreement with the theory and experimental results reported previously.[3]

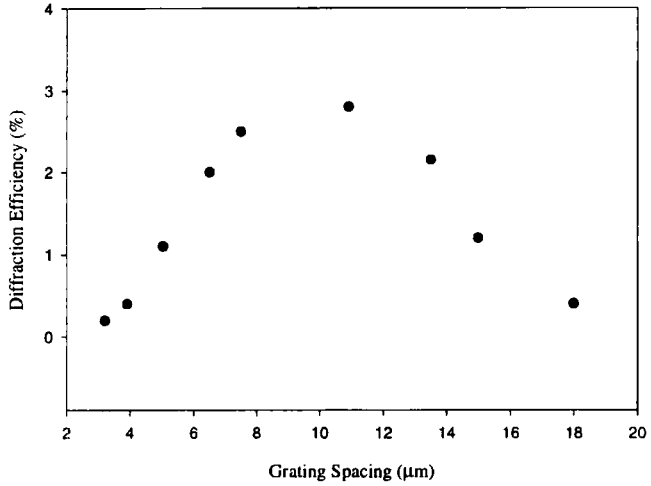

FIGURE 6: Dependence of the diffraction efficiency on the grating wavelength for permanent gratings formed in an undoped nematic film. The film thickness was 6 microns, P_{laser}=4 mW, λ = 448 nm, and V_{dc}=2V.

This study in thinner films shows that fairly high resolution gratings (>100 lines/mm) can be written in the undoped nematic film with low optical power density. In C60 doped or Methyl red dye doped nematic films, we have shown that similar gratings can be generated with much lower optical power density (200 $\mu W/cm^2$) for a 10 second exposure time (i.e. writing energy density of 2 mJ/cm^2).

Photo-Voltaic Effect in Methyl-Red Doped Nematic Films

As discussed in a previous section, the methyl-red doped homeotropically aligned nematic films present several unusual electro-optical effects not found in other doped (e.g. C60) samples, undoped samples, or in planar aligned methyl-red doped nematic films. In particular, we have observed the generation of a voltage across the cell boundary when the sample is illuminated by a low power linearly polarized argon-ion laser beam (we have observed similar effects with all the principle lines from the argon-ion laser). Figure 7 shows an example of the recorded DC voltage versus time across a 6 micron thick, homeotropically aligned, methyl-red doped, 5CB film, as measured from the input relative to the exit window. A sample illuminated with a 488 nm laser at an intensity of 1 mW/cm^2, elicited a peak voltage of about 6 mV. The polarity of the observed voltage was reversed if the incident direction of the light was reversed.

Such photo-voltaic effects have been observed in other liquid crystalline systems. In particular, S. Sato[14] reported observation of photo-induced voltage pulses in methyl-red doped MBBA films sandwiched between SnO_2 coated Pyrex glass plates, and also in 5CB nematic films. The actual mechanism(s) responsible for the photo-voltaic effects observed in our samples remain to be ascertained, but they may be similarly attributed to the photo-charge generation in the methyl-red doped nematic film, and

subsequent diffusion and redistribution of the ions with different mobilities. Exchanges of ions between the HTAB coated ITO electrodes and the doped nematic film could also be involved.

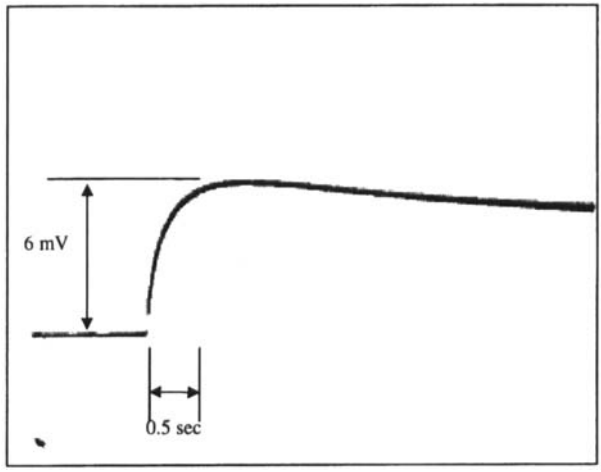

Figure 7: Oscilloscope trace of the DC voltage detected across a 6 micron thick homeotropically aligned 5CB film. Optical intensity used 1mW/cm^2;wavelength = 488 nm.

This new contribution to the optically induced DC fields within the nematic film may explain the unusually large wave mixing effect in these methyl-red doped films as noted in an earlier section. Figure 8 shows the self-diffraction efficiency versus the total input pump beam intensity with a small DC bias voltage of 0.2 volts along the direction of the photo-induced voltage. Using higher bias voltage, or applying the bias voltage in the reverse direction tends to diminish the effect, so 0.2 V appears to be the optimal bias voltage to use. Notice that even at sub mW/cm^2 optical intensity, one could still observe substantial diffraction. At a writing beam intensity of 2 mW/cm^2, the writing time (to achieve 50% of maximum) is found to be 150 ms. The writing time can be reduced with high intensity writing beams.

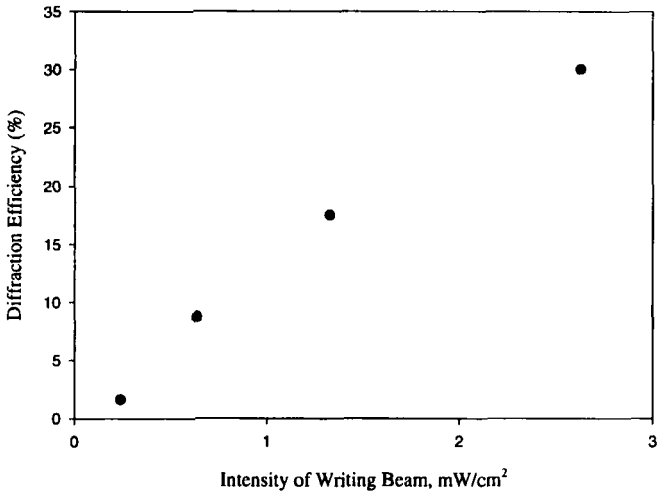

Figure 8: Self-diffraction efficiency as a function of input pump intensity in Methyl-red doped 5CB cell. Thickness: 6 μm; β=0; homeotropic alignment; grating constant = 12 μm; applied DC volt. = 0.2 volts.

CONCLUSION

In conclusion, we have presented an account of several nonlinear electro-optical wave mixing effects in nematic liquid crystals. It has been demonstrated that in thin samples under relatively low DC voltages, observable wave mixing effects such as self-diffraction can be created with very low input optical intensities (~10^2 μW/cm^2). Furthermore, the response times of these effects can be shortened to the millisecond regime. This sensitivity rivals those exhibited by conventional liquid crystal light valves. Phase aberration free amplification of a signal beam by a noisy pump beam has also been demonstrated. In addition, we have shown that permanent

gratings, down to a grating spacing of a few microns (>200 lines/mm), can be generated in these films. These newly observed effects are potentially useful for developing a new class of light valves or spatial light modulators, beam/image amplifiers, and/or other adaptive optics and coherent wave mixing devices.

Acknowledgements

The authors would like to thank M. Wood, M. Y. Shih, and P. Chen for their assistance in this work. The Air Force Phillips Laboratory and the Army Research Office provided support for this work. S. Slussarenko is supported by a U. S. Civilian Research and Development Foundation travel award.

References

[1.] E. V. Rudenko, A. V. Sukhov, "Optically induced spatial charge separation in nematic and the resultant orientational nonlinearity," *JETP*, **78**, 6, pp. 875-882, 1994.

[2.] I. C. Khoo, H. Li, Y. Liang, "Observation of orientational photorefractive effects in nematic liquid crystal," *Opt. Lett.*, **19**, pp. 1723-1725, 1994.

[3.] I. C. Khoo, "Orientational photorefractive effects in nematic liquid crystal films," *IEEE J. Quant. Elect.*, **32**, pp. 525-534, 1996.
(See also)
I. C. Khoo, "Optical dc field induced space charge fields and photorefractive-like holographic grating formation in nematic liquid crystals," *Mol. Cryst. Liq. Cryst.*, **282**, pp. 53-66, 1996.

[4.] G. P. Wiederrecht, B. A. Yoon, and M. R. Wasielewski, "High photorefractive gain in nematic liquid crystals doped with electron donor and acceptor molecules," *Science* **270**, pp. 1794-1797, 1995.

[5.] Brett Guenther, M. V. Wood, and I. C. Khoo, "Photorefractivity, phase conjugation and thermal wave mixing effects in the visible and near IR spectral region for dye and fullerene C60 doped nematic liquid crystals," *SPIE Proc.* **2854**, pp. 151-159, 1996.
(See also)
I. C. Khoo, Brett D. Guenther, and M. V. Wood, "Photorefractivity and holographic storage effects in fullerene C60 doped nematic liquid crystals," *Proc. Mat. Res. Soc.*, 1996.

[6.] I. C. Khoo, Brett Guenther, M. Wood, P. Chen, and M. Y. Shih, "Coherent beam amplification with photorefractive liquid crystal," *Opt. Lett.*, **22**, p. 1229, 1997.

[7.] P. Yeh, *Introduction to Photorefractive Nonlinear Optics*, Wiley-Interscience, New York, 1993.

[8.] F. P. Shaefer, Ed., *Dye Lasers*, Springer Verlag, Heidelberg 1974.

[9.] J. Mort, M. Mchonon, R. Ziolo, D. R. Huffman, and M.I. Ferguson, *Appl. Phys. Lett.* **60**, 1735, 1992.
See also
Y. Wang, *Nature*, **356**, p. 585, 1992.
See also
Y. Wang and L. T. Cheng, *J. Phys. Chem.*, **96**, 1530 1992.

[10.] I. C. Khoo, *Liquid Crystals: Physical Properties and Nonlinear Optical Phenomena*, Wiley Interscience, New York 1994.
See also
I. C. Khoo and S. T. Wu, *Optics and Nonlinear Optics of Liquid Crystals*, World Scientific, Singapore, 1993.

[11.] O. V. Garibyan, "Optical Phase Conjugation by microwatt power of reference waves via liquid crystal light valve," *Opt. Comm*, **38**, 67, 1981.

[12.] I. C. Khoo and T. H. Liu, *Phys. Rev.*, **A39**, pp. 4036-4044 1989.

[13.] Brett D. Guenther and I. C. Khoo, "Beam Amplification and clean-up with two and four wave mixing in photorefractive nematic liquid crystal films", *Proc. SPIE* **3143**, In Press (1997).

[14.] S. Sato, "Photovoltaic effects in MBBA cells containing organic dyes," *Jpn. J. Appl. Phys.*, **20**, p. 1989 (1981).
See also
L. K. Vistin, P. A. V. Kazlauskas, and S. Paeda, "Photoelectric effect in liquid crystals," *Sov. Phys. Dokl.*, **29**, p. 207, (1984).